Optofluidic FRET Lasers and Their Applications in Novel Photonic Devices and Biochemical Sensing

Mehdi Aas, Qiushu Chen, Alexandr Jonáš, Alper Kiraz, and Xudong Fan, *Member, IEEE*

***Abstract*—Incorporating fluorescence resonance energy transfer (FRET) into a laser cavity can increase the sensitivity of FRET-based biochemical sensors due to the nonlinear dependence of the lasing output on the FRET parameters. Here, we carry out a comprehensive theoretical analysis of optofluidic FRET lasers based on a Fabry–Pérot microcavity using a rate equation model. We compare conceptually distinct cases of donor and acceptor molecules diffusing freely in a bulk solution versus molecules connected by a fixed-length linker and show that the latter arrangement is especially well suited for sensing of low-concentration analytes. By comparing FRET lasing-based sensors with conventional FRET sensors, we show that for optimal pump fluence and FRET-pair concentration, FRET lasing can lead to more than 100-fold enhancement in detection sensitivities of conformational changes in the Förster radius range. We also show that for optimal experimental conditions, donor and acceptor emission intensities become over 20-fold more sensitive to FRET-pair concentration changes in the presence of FRET lasing. We study the dependence of the sensitivity enhancement on the cavity Q-factor. We show that the highest enhancements can be obtained for Q-factors between 10^4–10^6, and enhancement values decrease for Q-factors above 10^6 due to the radiative energy transfer in the cavity.**

***Index Terms*—Biophotonics, biophysics, biosensors, fluorescence, lasers, nonlinear optics, optical resonators.**

I. Introduction

NON-RADIATIVE fluorescence resonance energy transfer (FRET) between a pair of donor and acceptor chromophores displaying sufficient spectral overlap can serve as a precise ruler to measure the distance between the two chromophores with atomic-scale resolution. Working range of FRET is limited to chromophore spacings less than 10 nm, typical size of large biomolecules such as proteins and nucleic acids. Therefore, FRET is commonly used in biological and biochemical sensing for studying conformational changes or quantifying interactions between different biomolecules and molecular complexes in live cells [1], [2]. When biomolecules labeled with the donor and acceptor dyes undergo a conformational change or binding/unbinding process, the distance between the donor and acceptor changes, resulting in a change in the donor and acceptor emission intensity which constitutes the FRET signal. In addition to sensing applications, FRET has also been employed as an alternative mechanism for pumping laser gain media [3], [4]. In these demonstrations, donor and acceptor molecules are mixed together in a liquid or solid host matrix. Subsequently, the donor molecules are directly pumped using an external source of energy. Excited donor molecules then transfer their energy to acceptor molecules that emit coherent laser light. Typically, the distances between the donor and acceptor molecules are randomly distributed and determined statistically by the donor and acceptor concentrations.

Optofluidic lasers have recently emerged as a promising technology for developing novel photonic devices and highly sensitive biochemical sensors [5]–[7]. Optofluidic lasers integrate optical microcavities and gain media into liquid environments contained within suitable microfluidic circuits or chips. On the photonic device side, they exploit flexibility of material characteristics and geometrical shape of liquids for creating miniaturized light sources embedded directly on a chip. On the biosensing side, optofluidic lasers take advantage of a fully-biocompatible aqueous working environment. Analytes under study, which form laser gain media, can be directly placed within the optical mode volume. Thus, amplified lasing emission rather than ordinary spontaneous fluorescence serves as the sensing signal. Due to the optical feedback provided by the cavity, a small change in the gain medium induced by underlying biological processes is significantly amplified, leading to a dramatic change in the laser output characteristics.

An optofluidic FRET laser can be constructed by placing a suitable pair of FRET acceptor and donor dyes inside a laser cavity or, more precisely, within the laser mode volume. Changes in FRET efficiency brought about by modulation of the separation distance between the donor and acceptor molecules will then translate into modulation of the laser output energy. Recent experiments demonstrated that the same underlying biological process or the same change of FRET efficiency can result in changes of the lasing emission intensity from the donor and/or the acceptor that are orders of magnitude larger than those observed in conventional FRET based on spontaneous fluorescence [8]–[11]. Furthermore, besides intensity and polarization of the emitted light, laser output consists of many more parameters that can be monitored and serve as a measurement signal, such as the lasing threshold, lasing efficiency, and lasing mode spatial profile. Therefore, optofluidic FRET lasers provide a powerful complementary technology to analyze minute

Manuscript received June 27, 2015; revised September 02, 2015; accepted September 03, 2015. Date of publication September 11, 2015; date of current version October 30, 2015. This work was supported by the National Institutes of Health under Grant 1R21EB016783. The work of A. Kiraz was supported by a Fulbright Fellowship. *(Corresponding authors: Xudong Fan and Alper Kiraz.)*

M. Aas is with the Department of Physics, Koç University, Istanbul 34450, Turkey (e-mail: maas@ku.edu.tr).

Q. Chen and X. Fan are with the Department of Biomedical Engineering, University of Michigan, Ann Arbor, MI 48109 USA (e-mail: qschen@umich.edu; xsfan@umich.edu).

A. Jonáš is with the Department of Physics, Istanbul Technical University, Istanbul 34469, Turkey (e-mail: ajonas@itu.edu.tr).

A. Kiraz is with the Department of Physics, Koç University, Istanbul 34450, Turkey, and also with the Department of Biomedical Engineering, University of Michigan, Ann Arbor, MI 48109 USA (e-mail: akiraz@ku.edu.tr).

Color versions of one or more of the figures in this paper are available online at http://ieeexplore.ieee.org.

Digital Object Identifier 10.1109/JSTQE.2015.2477397

changes in biomolecules that may otherwise remain indistinguishable with conventional FRET.

Optofluidic FRET lasers also open the door for developing new types of sources of coherent light. With recent advances in nanotechnology and biotechnology, the number and position of the donor and acceptor molecules located within the laser mode volume can be precisely controlled and modulated with sub-nanometer spatial resolution. Therefore, overall FRET efficiency is no longer dependent upon the bulk concentrations of the donor and acceptor molecules, and high FRET efficiencies can be maintained even at the single-molecular level [12], [13]. Recently, lasing from a single-layer gain medium containing orders of magnitude fewer gain molecules than the conventional bulk active media has been demonstrated [14]. Therefore, it is imaginable that lasing from only a few gain molecules might be achievable [14], [15], in which the FRET pumping mechanism is strongly preferable to the direct optical excitation in order to achieve higher pumping efficiency [15].

The purpose of this paper is to carry out a comprehensive analysis of optofluidic FRET lasers using the framework of rate equations for the excited state populations of the donor and acceptor molecules and the corresponding donor and acceptor photon densities. We aim to provide both fundamental understanding of FRET lasers and strategies for constructing optimized FRET lasers for better sensing and photonic performances. To keep the manuscript self-contained, we start with the description and analysis of FRET lasers in which the donor and acceptor molecules are randomly distributed in bulk solution contained within a Fabry–Pérot cavity. Subsequently, we focus on FRET lasers based on molecular constructs linking the donor and acceptor dyes at a predetermined constant distance and stoichiometric ratio. We study the performance of FRET lasers as a function of concentration of the donor and acceptor molecules in the laser cavity, pump fluence, and intermolecular distance between the acceptor and donor molecules. For lasers containing linked donor/acceptor pairs, we analyze the sensitivity of the FRET output signal to changes of donor/acceptor intermolecular spacing and concentration of linked complexes in the laser cavity. We show that when the FRET lasers are operated in an optimal range of pump fluences and linked complex concentrations, for linker lengths around the Förster radius, more than 100 times enhancement can be achieved in output signal sensitivity in comparison to the conventional FRET measurements based on spontaneous fluorescence.

A. Rate Equation Model

Our rate equations are based on those developed previously for a dye laser consisting of a single-dye gain medium [16]. These equations have been expanded to account for the presence of a saturable absorber dye acting as an energy acceptor which is radiatively coupled to the donor dye [17], [18]. Moreover, additional terms describing FRET-based non-radiative energy transfer between the donor and acceptor molecules have been included [19]. The complete energy level diagram of the gain medium and transitions considered in our model is shown in Fig. 1(a).

The coupled differential equations used to describe the population dynamics of FRET dye pair serving as the laser gain medium read as:

$$\begin{aligned}\frac{dn_d(t)}{dt} &= I_p(t)\,\sigma_{pd}\left[N_d - n_d(t)\right] - \frac{\sigma_{edd}c}{\eta}n_d(t)\,q_d(t)\\ &\quad + \frac{\sigma_{add}c}{\eta}\left[N_d - n_d(t)\right]q_d(t) - \frac{n_d(t)}{\tau_d}\\ &\quad - k_F n_d(t), \qquad (1)\\ \frac{dq_d(t)}{dt} &= \frac{Fc}{\eta}\left[\sigma_{edd} - \sigma_{1\mathrm{dd}}\right]n_d(t)\,q_d(t) + \frac{Fc}{\eta V}\sigma_{edd}n_d(t)\\ &\quad - \frac{Fc}{\eta}\sigma_{add}\left[N_d - n_d(t)\right]q_d(t) - \frac{q_d(t)}{\tau_{cd}}\\ &\quad + \frac{Fc}{\eta}\sigma_{ead}n_a(t)\,q_d(t) - \frac{Fc}{\eta}\sigma_{1ad}n_a(t)\,q_d(t)\\ &\quad - \frac{Fc}{\eta}\sigma_{aad}\left[N_a - n_a(t)\right]q_d(t), \qquad (2)\\ \frac{dn_a(t)}{dt} &= I_p(t)\,\sigma_{pa}\left[N_a - n_a(t)\right] - \frac{\sigma_{ead}c}{\eta}n_a(t)\,q_d(t)\\ &\quad - \frac{n_a(t)}{\tau_a} + \frac{\sigma_{aad}c}{\eta}\left[N_a - n_a(t)\right]q_d(t)\\ &\quad - \frac{\sigma_{eaa}c}{\eta}n_a(t)\,q_a(t) + k_F n_d(t)\\ &\quad + \frac{\sigma_{aaa}c}{\eta}\left[N_a - n_a(t)\right]q_a(t), \qquad (3)\\ \frac{dq_a(t)}{dt} &= \frac{Fc}{\eta}\left[\sigma_{eaa} - \sigma_{1aa}\right]n_a(t)\,q_a(t) + \frac{Fc}{\eta V}\sigma_{eaa}n_a(t)\\ &\quad - \frac{Fc}{\eta}\sigma_{aaa}\left[N_a - n_a(t)\right]q_a(t) - \frac{q_a(t)}{\tau_{ca}}. \qquad (4)\end{aligned}$$

In these equations, n_d, n_a and q_d, q_a describe the spatially averaged, time-dependent densities of the dye molecules in the first excited states S_{1d}, S_{1a}, and the time-dependent photon densities at a single lasing line for the donor and acceptor dyes, respectively. σ_{pd}, σ_{pa}, σ_{edd}, σ_{eaa}, σ_{ead}, σ_{add}, $\sigma_{1\mathrm{dd}}$, σ_{1aa}, σ_{1ad}, σ_{aad}, and σ_{aaa} describe different absorption and emission cross-sections of the donor and acceptor molecules, as summarized in Table I. $I_p(t)$ is the time-dependent pump intensity in the units of $\mathrm{photons}/(\mathrm{cm}^2 \cdot \mathrm{s})$, N_d and N_a are the total concentrations of donor and acceptor molecules, and k_F is the FRET rate. η is the refractive index of the medium. τ_d and τ_a are the fluorescence lifetimes for donor and acceptor molecules, respectively. τ_{cd} and τ_{ca} denote cavity decay times at the donor and acceptor lasing wavelengths (λ_d and λ_a), respectively. We calculate τ_{cd} and τ_{ca} using the general relation $\tau_c(\lambda) = Q_0\lambda/(2\pi c)$ where Q_0 denotes the quality factor (Q-factor) of an empty cavity and c denotes the speed of light in vacuum. V is the mode volume and F is the fraction of the mode volume occupied by the dye molecules. The second terms on the right-hand side of Eqs. (2) and (4) describe the photon noise generation or spontaneous emission, indicating the fraction of spontaneously emitted photons coupled into the lasing modes. In accordance with Ref. [16], our calculations are insensitive to the absolute

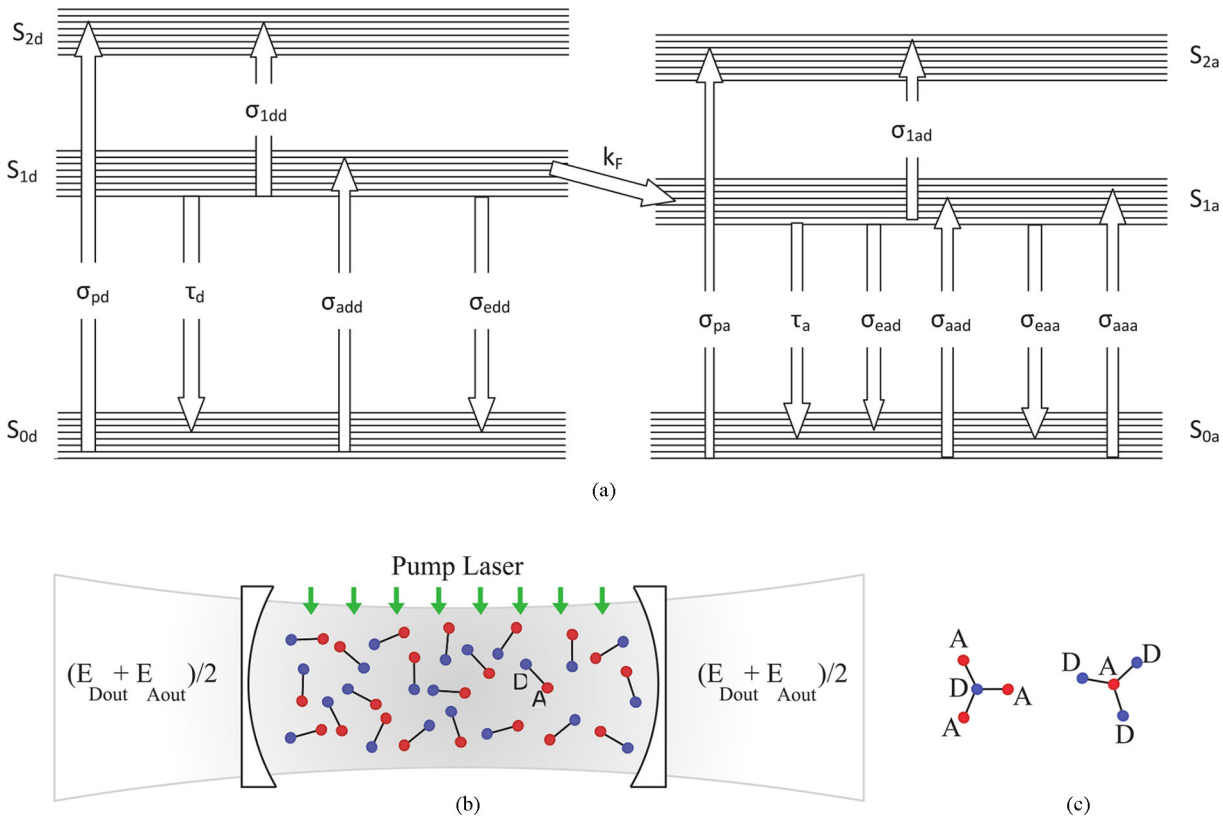

Fig. 1. (a) Schematic diagram of molecular energy levels for a pair of donor and acceptor dyes showing the lowest three singlet energy levels and their sub-levels for each dye. All relevant electronic transitions that are included in our rate equation model are identified by absorption and emission cross sections specified on the arrows with appropriate transition direction. Non-radiative FRET is assumed to happen between S_{1d} and S_{1a} energy bands. Definitions of individual symbols are given in the text. (b) A simplified Fabry–Pérot laser cavity with two identical output couplers and linked donor/acceptor pairs representing FRET-based active medium. (c) Schematics of molecular constructs with a constant donor–acceptor distance containing one donor linked to three acceptors (1D−3A) or three donors linked to one acceptor (3D−1A).

value of the coefficients in these spontaneous emission terms. In this paper, we assume donor and acceptor lasing at a single wavelength (optical mode), although our rate equation model can be extended to multi-mode lasing by adding differential equations describing the rates of changes for photon densities at these additional optical modes [16].

In this paper, we consider gain medium placed into a simple rectangular Fabry–Pérot optical cavity [see Fig. 1(b)]. Assuming identical out-coupling coefficients for both mirrors of the cavity, the time-dependent total output power emitted from both sides of the cavity from the donor and acceptor dyes can be calculated using the following equations [20]:

$$P_{\text{Dout}}(t) = \frac{hcq_d(t)V_p}{\lambda_d \tau_{cd}}, \tag{5}$$

and

$$P_{\text{Aout}}(t) = \frac{hcq_a(t)V_p}{\lambda_a \tau_{ca}}, \tag{6}$$

where V_p is the volume of the pumped region of the laser gain medium that can be determined from the pumping beam profile and its illumination geometry and h is the Planck constant. The total output energy of the donor and acceptor pulses (E_{Dout} and E_{Aout}, respectively), can be subsequently calculated by integrating $P_{\text{Dout}}(t)$ and $P_{\text{Aout}}(t)$ over time. We consider a uniform profile of the pump beam illuminating the gain medium from the top of the Fabry–Pérot cavity [see Fig. 1(b)]. For simplicity, we further assume that the electromagnetic mode density inside the cavity is uniform and, thus, the mode volume can be represented as $V = dwl$, where d, w, and l are the spatial extents of the electromagnetic mode in individual dimensions. The pump beam penetration depth into the active lasing medium is $d_p = 1/(N_d\sigma_{pd} + N_a\sigma_{pa})$. The condition below can be used for determining the value of V_p depending on the values of d and d_p:

$$V_p = \min(FV, Fd_pV/d). \tag{7}$$

FRET efficiency, k_F, is influenced by the actual configuration of the donor and acceptor molecules. For the case of the donor and acceptor molecules dissolved in a liquid medium, moving freely relative to each other, k_F is essentially a time-dependent parameter. Depending on the solvent viscosity and the lifetime of the donor excited state, time dependence of k_F can be determined using different methods [21]. For typical organic dyes with large molecules dissolved in typical solvents like ethanol or water at concentrations less than a few mM, the diffusion lengths of the donor and acceptor dye molecules during the donor decay time (typically a few nanoseconds) are much smaller than the average separation distance between the donor and acceptor

TABLE I
DESCRIPTIONS AND NUMERICAL VALUES OF THE CONSTANTS USED IN THE RATE EQUATION MODEL [19]

Constant	Description	Numeric Value
σ_{pd}	Donor absorption cross section at the pump wavelength	3.42×10^{-16} cm^2
σ_{pa}	Acceptor absorption cross section at the pump wavelength	0.05×10^{-16} cm^2
σ_{edd}	Donor stimulated emission cross section at λ_d	3.78×10^{-16} cm^2
σ_{eaa}	Acceptor stimulated emission cross section at λ_a	6.9×10^{-16} cm^2
σ_{ead}	Acceptor stimulated emission cross section at λ_d	0.036×10^{-16} cm^2
σ_{add}	Donor absorption cross section at λ_d	1.00×10^{-16} cm^2
$\sigma_{1\mathrm{dd}}$	Excited state absorption cross section of donor molecules at λ_d	0.4×10^{-16} cm^2
σ_{1aa}	Excited state absorption cross section of acceptor molecules at λ_a	2.00×10^{-16} cm^2
σ_{1ad}	Excited state absorption cross section of acceptor molecules at λ_d	1.30×10^{-16} cm^2
σ_{aad}	Acceptor absorption cross section at λ_d	0.156×10^{-16} cm^2
σ_{aaa}	Acceptor absorption cross section at λ_a	1.00×10^{-16} cm^2
η	Refractive index of the medium	1.33
τ_d	Fluorescence lifetime of donor molecules	4 ns
τ_a	Fluorescence lifetime of acceptor molecules	3.3 ns
τ_{cd}	Fluorescence lifetime of cavity at λ_d	$Q_0\lambda_d/(2\pi c)$
τ_{ca}	Fluorescence lifetime of cavity at λ_a	$Q_0\lambda_a/(2\pi c)$
λ_d	Donor lasing wavelength	560 nm
λ_a	Acceptor lasing wavelength	655 nm
R_0	Förster radius	6.1 nm
Q_0	Empty cavity Q-factor	10^6
F	Fraction of mode volume occupied by the dye molecules	1
d	Depth of the electromagnetic mode	30 μm
w	Width of the electromagnetic mode	30 μm
l	Length of the electromagnetic mode	30 μm
V	Volume of the electromagnetic mode	dwl
Δt	Pump laser pulsewidth	5 ns
c	Speed of light in vacuum	3×10^{10} cm/s
h	Planck's constant	$6.62606957 \times 10^{-34}$ J $\cdot$ s

molecules. In such a case, donor and acceptor molecules can be assumed to be at fixed positions, and an average energy transfer rate can be obtained using [22]:

$$k_F = \frac{1}{\tau_d}\left(\frac{\sqrt{\pi}\beta e^{\beta^2}\operatorname{erfc}(\beta)}{1-\sqrt{\pi}\beta e^{\beta^2}\operatorname{erfc}(\beta)}\right), \tag{8}$$

where erfc is the complementary error function and $\beta = \frac{2}{3}\pi^{3/2}N_a R_0^3$.

For the case that the donor and acceptor molecules are connected to each other through a linker molecule which ensures a fixed separation distance [12], [14], and under the condition that the overall concentration of linked complexes is low enough so that the donors/acceptors in individual complexes do not transfer energy to other donors/acceptors in the neighboring complexes, k_F can be determined using the basic transfer rate, k_{F0}, of an isolated donor–acceptor dye pair:

$$k_{F0} = \frac{1}{\tau_d}\left(\frac{R_0}{R}\right)^6, \tag{9}$$

where R and R_0 are the dye separation distance and the Förster radius of the donor/acceptor FRET pair, respectively.

When an individual linked dye complex contains just one donor and one acceptor molecule, the rate of FRET is simply $k_F(\mathrm{1D–1A}) = k_{F0}$. However, when the ratio of donors and acceptors in an individual complex is not unity, k_F will be equal to different fractions of k_{F0}, depending on the actual number of donors and acceptors in the complex. In Fig. 1(c), two distinct linked complexes considered in this paper are shown. The first complex has one donor and three identical acceptors located at equal distances from the donor, 1D–3A, and the second complex has one acceptor and three identical donors located at equal distances from the acceptor, 3D–1A. For 1D–3A, the transfer rate increases threefold and we have $k_F(\mathrm{1D–3A}) = 3k_{F0}$ whereas for 3D–1A, the transfer rate for each donor is limited to one acceptor and, thus, $k_F(\mathrm{3D–1A}) = k_{F0}$.

In the simulations presented in this article, we study a model system for optofluidic FRET lasing which consists of Rhodamine 6G (R6G) as the donor and Acid Blue 7 (AB7) as the acceptor. The values of various transition cross-sections and lifetimes describing this FRET pair are summarized in Table I together with other relevant simulation parameters. The coupled rate equations (1)–(4) are numerically solved for different excitation pump profiles, $I_p(t)$, using MATLAB [23]

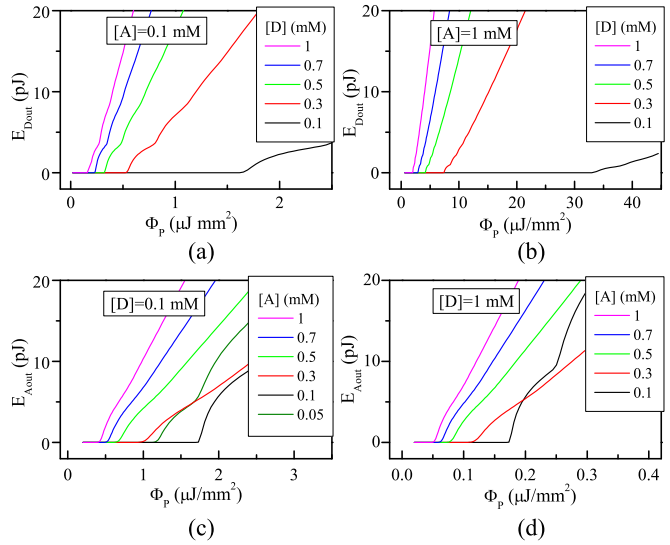

Fig. 2. Total output emission energy E_{Dout}, E_{Aout} from bulk solutions of R6G/AB7 FRET pair as a function of the pump fluence, Φ_P. (a) Donor lasing with fixed acceptor concentration [A] = 0.1 mM and varying donor concentration [D] = 1 to 0.1 mM. (b) Donor lasing with fixed acceptor concentration [A] = 1 mM and varying donor concentration [D] = 1 to 0.1 mM. (c) Acceptor lasing with fixed donor concentration [D] = 0.1 mM and varying acceptor concentration [A] = 1 to 0.05 mM. (d) Acceptor lasing with fixed donor concentration [D] = 1 mM and varying acceptor concentration [A] = 1 to 0.1 mM.

stiff ODE solver ODE15s for varying donor/acceptor molecular arrangements and concentrations. We assume a Gaussian temporal profile of pump intensity, $I_p = I_{p0} \cdot \exp(-4 \cdot \ln 2 \cdot [(t - t_0)/\Delta t]^2)$, with $\Delta t = 5$ ns or $\Delta t = 50$ μs pulsewidth. Peak intensity of the pulse (I_{p0}) is then calculated using $I_{p0} = \frac{0.94\lambda_p}{hc\Delta t}\Phi_p$, where Φ_p is the pulse energy fluence and λ_P is the pump wavelength. At pump intensities above the lasing threshold, multiple lasing peaks are observed in the temporal profiles of the donor and acceptor emissions due to Q-switching in the gain medium [17]–[19]. When reporting the total output lasing energy for a given combination of system parameters (pump fluence, dye concentration, spacing between donor and acceptor), we always use integral values including all output pulses excited with a single pump pulse.

II. Threshold Behavior of Bulk FRET Lasers

We begin our analysis of optofluidic FRET lasers by characterizing the main properties of donor and acceptor lasing for the case of the donor and acceptor molecules dissolved in a bulk solution, without being linked at a fixed separation distance. Fig. 2 shows the total output energy of donor and acceptor emissions, E_{Dout} and E_{Aout}, calculated for a wide range of donor and acceptor concentrations ([D] and [A]) as a function of the pump fluence (Φ_P). In all studied cases, the slope of the curves changes abruptly at a certain threshold value of Φ_P that indicates the onset of lasing. In several cases (such as donor lasing at [A] = 0.1 mM and acceptor lasing at [D] = 0.1 mM), the output energy curve displays ripples for Φ_P values larger than the lasing threshold. This is a consequence of multiple lasing peaks appearing in the temporal profile of the output power induced by the gain Q-switching [19]. Fig. 3 shows detailed

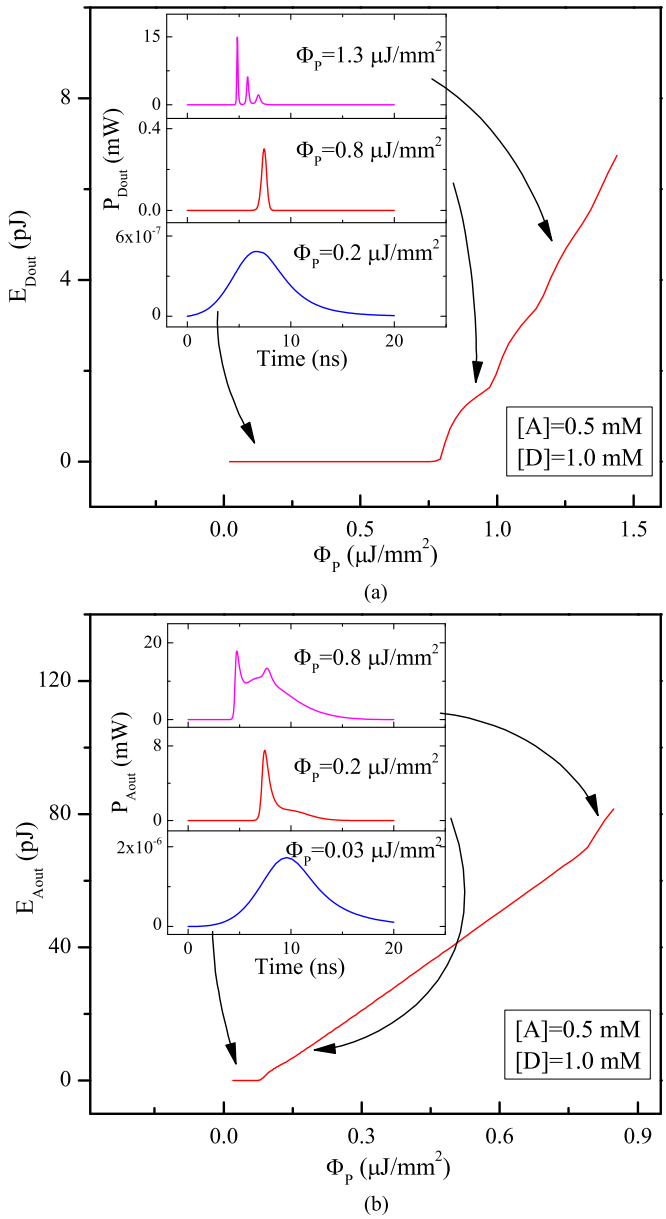

Fig. 3. Gain Q-switching in optofluidic FRET lasers. (a) Total output emission energy E_{Dout} from the donor as a function of Φ_P. Insets show the time profiles of the donor emission power before reaching the lasing threshold at $\Phi_{\mathrm{P}} = 0.2\ \mu\mathrm{J/mm}^2$, shortly after crossing the threshold at $\Phi_{\mathrm{P}} = 0.8\ \mu\mathrm{J/mm}^2$ (a single output pulse), and well above the threshold at $\Phi_{\mathrm{P}} = 1.3\ \mu\mathrm{J/mm}^2$ (three output pulses corresponding to the third ripple in the output energy curve). (b) Total output emission energy E_{Aout} from the acceptor as a function of Φ_P. Insets show the time profiles of the acceptor emission power before reaching the lasing threshold at $\Phi_{\mathrm{P}} = 0.03\ \mu\mathrm{J/mm}^2$, shortly after crossing the threshold at $\Phi_{\mathrm{P}} = 0.2\ \mu\mathrm{J/mm}^2$ (a single output pulse), and well above the threshold at $\Phi_{\mathrm{P}} = 0.8\ \mu\mathrm{J/mm}^2$ (two output pulses corresponding to the second ripple in the output energy curve).

views of the donor [see Fig. 3(a)] and acceptor [see Fig. 3(b)] output energy curves. Insets in the respective subfigures illustrate the temporal profiles of the donor and acceptor output emission power $P_{\mathrm{Dout}}(t)$ and $P_{\mathrm{Aout}}(t)$ for different Φ_P values. Temporal narrowing of the output pulse and appearance of multiple after-pulses with increasing Φ_P are clearly visible for both donor and acceptor laser emissions.

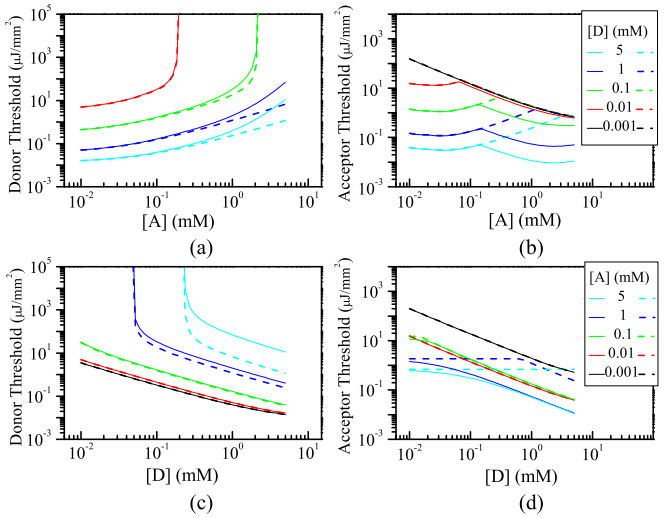

Fig. 4. Threshold Φ_P of bulk FRET lasing of (a) donor and (b) acceptor as a function of acceptor concentration [A] for several fixed donor concentrations [D]. Threshold Φ_P of bulk FRET lasing for (c) donor and (d) acceptor as a function of donor concentration [D] for several fixed acceptor concentrations [A]. Solid and dashed curves in (a)–(d) indicate calculations performed assuming active (k_F calculated using Eq. (8)) and inactive ($k_F = 0$) FRET channels, respectively. The figure legends for (a) and (c) are shown in (b) and (d), respectively.

Threshold values of Φ_P for donor and acceptor lasing extracted from the output energy curves similar to those presented in Fig. 2 are shown in Fig. 4 for different donor and acceptor concentrations. In order to elucidate the effect of the FRET channel on the overall behavior of the optofluidic lasers using a mixture of two fluorescent dyes as the laser gain medium, we also perform calculations in which the FRET transition is turned OFF by setting $k_F = 0$. These cases are indicated by dashed lines in Fig. 4. With the inactive FRET channel, the donor and acceptor dyes can still couple radiatively through the cavity-enhanced energy transfer (CET) in which the resonant photons emitted by the donor and circulating in the laser cavity are reabsorbed by the acceptor molecules [24]–[26].

Fig. 4(a) shows the threshold Φ_P for donor lasing as a function of acceptor concentration ([A] = 0.01–5 mM) for different fixed donor concentrations ([D] = 0.01, 0.1, 1, 5 mM). For [D] between 1–5 mM, donor lasing is observed for all values of [A], while for [D] = 0.01 mM and [D] = 0.1 mM, donor lasing is not observed for [A] $>$ 0.2 mM and [A] $>$ 2 mM, respectively, due to the high absorption of acceptor dye in donor emission wavelength and nonradiative FRET depletion of the excited population of the donor to the acceptor dye. Comparison of the solid and dashed lines in the donor threshold curves obtained for [D] = 0.01 and 0.1 mM suggests that for these cases, FRET channel does not play a significant role and the donor population is depleted mainly by the radiative CET to the acceptor molecules. For the selected range of [A], donor lasing is not observed at all for [D] $\leq$ 0.001 mM. For high donor and acceptor concentrations ([D], [A] $>$ 1 mM), donor lasing threshold values obtained with active FRET channel are higher than those corresponding to the inactive FRET case (i.e., $k_F = 0$) due to the additional depletion of the excited donor molecules by the FRET channel.

Threshold values of Φ_P for acceptor lasing are plotted in Fig. 4(b) as a function of [A] for different fixed values of [D]. In general, higher values of [D] lead to lowering of the acceptor lasing threshold due to more efficient pumping of the acceptor. In the active FRET case (solid curves), dependence of the acceptor lasing threshold on [A] displays two different trends. When donor lasing is dominant, i.e., the donor starts lasing at a lower pump fluence than the acceptor (high [D] and low [A]), acceptor lasing threshold shows little change or even a slight increase with increasing [A]. In contrast, when acceptor lasing becomes dominant (high [A]), acceptor lasing threshold decreases with increasing [A]. The effect of FRET can be clearly observed for high [D] and [A] (green, blue and cyan curves for [A] $>$ 0.2 mM), when the typical distance between the donor and acceptor molecules becomes comparable to the Förster radius R_0. In this regime, acceptor lasing threshold with active FRET channel lies significantly below the corresponding value for the inactive FRET case, indicating efficient pumping of acceptor molecules via the non-radiative energy transfer.

Fig. 4(c) shows the dependence of the donor lasing threshold on [D] for different fixed values of [A]. As expected, the donor lasing threshold decreases with increasing [D] and decreasing [A], corresponding to higher gain and lower loss, respectively. For high acceptor concentrations of [A] = 1 mM and [A] = 5 mM, donor lasing is completely quenched for [D] $\lesssim$ 0.05 mM and [D] $\lesssim$ 0.2 mM, respectively. The effect of the FRET channel on the donor lasing threshold curves is well visible for [A] = 1–5 mM (compare solid and dashed curves in blue and cyan color). In this range of acceptor concentrations, the presence of the FRET channel leads to higher overall losses for donor lasing, and, therefore, an increase in the donor lasing threshold.

In Fig. 4(d), the acceptor lasing threshold is plotted as a function of [D] for different fixed values of [A]. With increasing [D], acceptor molecules are pumped more efficiently via the FRET and/or CET channels. This leads to a decrease in the acceptor lasing threshold. The effect of FRET on the acceptor lasing threshold is clearly visible for [A] = 1–5 mM (compare corresponding solid and dashed curves). At these acceptor concentrations, donor and acceptor molecules are sufficiently close to each other and, thus, the presence of FRET leads to more efficient acceptor pumping that lowers the acceptor lasing threshold.

In summary, the analysis of lasing threshold presented in Fig. 4 indicates that in the case of bulk solutions of donor and acceptor, the efficiency of FRET and, therefore, its contribution to the acceptor pumping is determined solely by the dye concentration. For sufficiently high values of [A] and [D], average distance between the donor and acceptor molecules approaches the Förster radius R_0 of the dye pair. Consequently, FRET rate increases dramatically and non-radiative energy transfer becomes the dominant mechanism for acceptor pumping.

III. Threshold Behavior of Molecularly Linked FRET Pair Lasers

After analyzing optofluidic lasers based on energy transfer between donor and acceptor molecules dissolved in bulk solutions, we focus our attention on the situation in which the donor and acceptor molecules are connected to each other using a

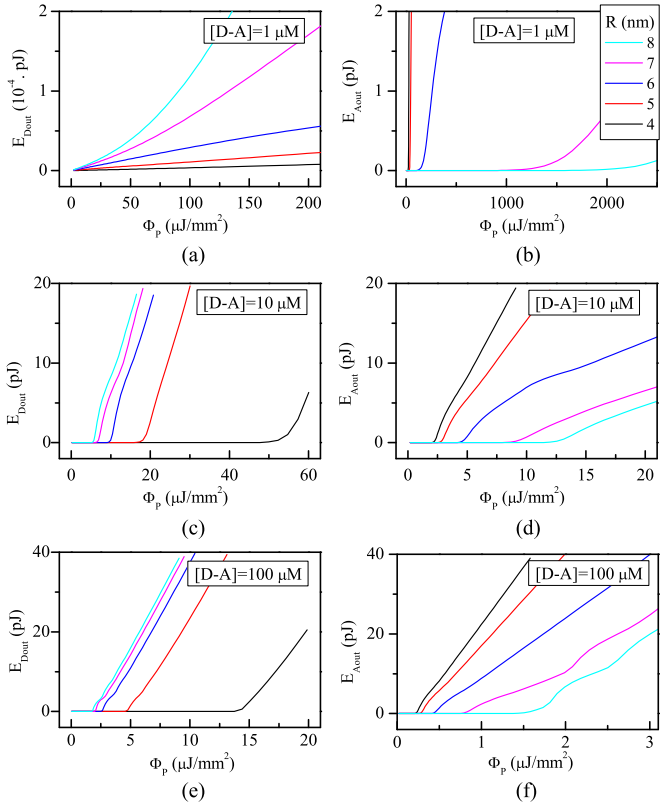

Fig. 5. Total output emission energy E_{Dout}, E_{Aout} from molecularly linked FRET pair R6G/AB7 (denoted as D–A) as a function of Φ_P for different [D–A] values and linker lengths R. In (a), no lasing is observed in donor emission. Plot legend shown in (b) applies to all figures (a)–(f).

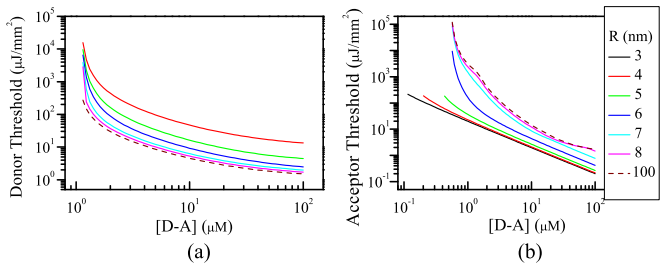

Fig. 6. (a) Donor lasing threshold as a function of [D–A] for different linker lengths R. (b) Acceptor lasing threshold as a function of [D–A] for different linker lengths R.

molecular linker of a fixed length. In this situation, transfer rate k_F describing the efficiency of FRET is a constant independent of the total concentration of linked complexes in the laser gain medium. Fig. 5 shows the total output energies of the donor and acceptor emissions E_{Dout} and E_{Aout} calculated for the case of a molecularly linked FRET pair (denoted as D–A) for different concentrations of the linked dye complex ([D–A]) and linker lengths (R), as a function of Φ_P. Threshold values of Φ_P obtained from such output energy curves are plotted in Fig. 6. With decreasing R which translates into increasing k_F, donor and acceptor lasing threshold fluences are observed to increase and decrease, respectively. In contrast to the bulk case, for the linked case, FRET can be the dominant energy transfer mechanism even at low [D–A] values $\sim 1\ \mu$M, provided that R is comparable to the Förster radius, which is $R_0 = 6.1$ nm for the selected FRET pair. In order to quantify relative contributions of FRET and CET to lasing, we calculated lasing thresholds for a very long linker ($R = 100$ nm) where CET becomes the dominant energy transfer mechanism; these calculations are shown as dashed curves in Fig. 6(a) and (b). For all [D–A] values studied in Fig. 6, when R is comparable to or smaller than R_0, the donor lasing threshold fluences become significantly higher and the acceptor lasing threshold fluences become significantly lower than the corresponding values for the very long linker case, which are determined solely by CET. Hence, for the range of [D–A] values under study and linker lengths $R \lesssim R_0$, FRET is the dominant mechanism for determining the donor and acceptor lasing properties.

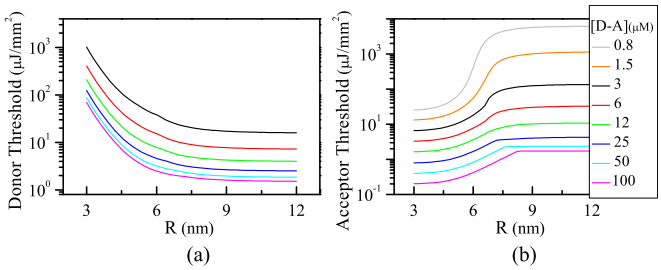

Fig. 7. (a) Donor lasing threshold as a function of linker length R for different [D–A] values. (b) Acceptor lasing threshold as a function of linker length R for different [D–A] values.

Fig. 7 shows the donor and acceptor lasing threshold fluences calculated for a molecularly linked FRET pair as a function of R for different [D–A] values. For [D–A] $< 3\ \mu$M, donor lasing is not observed. Hence, in Fig. 7, donor lasing threshold values are plotted for [D–A] ranging between 3–100 μM while acceptor lasing threshold values are plotted for [D–A] ranging between 0.8–100 μM. Donor and acceptor threshold fluences follow different dependencies on R. For the values of R much smaller than R_0, donor energy is almost fully transferred to the acceptor via the very efficient FRET channel. This leads to a very fast depletion of the excited donor molecules, preventing donor lasing. Hence, donor lasing threshold increases indefinitely as $R \to 0$. In this regime, acceptor lasing threshold is determined solely by the inherent properties of the acceptor dye, similarly to the case of lasing with a single-dye gain medium. When R is much larger than R_0, donor and acceptor lasing properties follow the trends observed in the bulk lasing case. Thus, for the concentrations considered in Fig. 7, CET becomes the dominant energy transfer mechanism. In this limit, donor and acceptor lasing thresholds do not depend on R.

IV. Sensitivity of Detection for Conformational Changes in Linked FRET Pair Biocomplexes

Analysis performed in the previous section has shown that in the case of a molecularly linked donor–acceptor dye pair, FRET dominates over CET in providing pump energy for lasing of the acceptor dye molecules provided that $R \lesssim R_0$. Hence, this linked-dye configuration is much more suitable for molecular

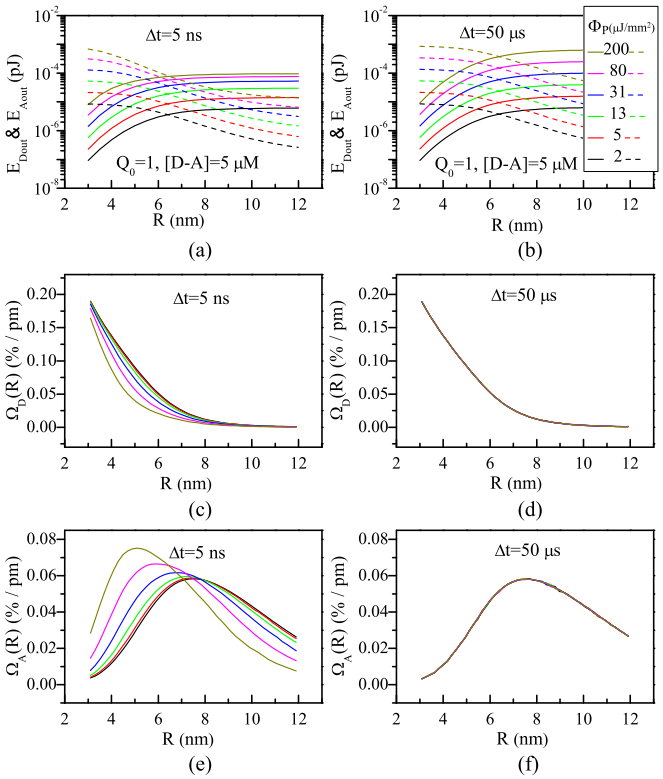

Fig. 8. Performance of FRET-based biosensors using spontaneous fluorescence emission for [D–A] $= 5\ \mu$M. Donor (solid curves) and acceptor (dashed curves) fluorescence emission energy from linked donor/acceptor pairs versus R at different values of Φ_P for excitation pulsewidth of (a) $\Delta t = 5$ ns and (b) $\Delta t = 50\ \mu$s. Donor emission sensitivity to linker length ($\Omega_D(R)$) versus R for FRET emission from linked donor/acceptor pairs at different values of Φ_P for excitation pulsewidth of (c) $\Delta t = 5$ ns and (d) $\Delta t = 50\ \mu$s. Acceptor emission sensitivity to linker length ($\Omega_A(R)$) versus R for FRET emission from linked donor/acceptor pairs at different values of Φ_P for excitation pulsewidth of (e) $\Delta t = 5$ ns and (f) $\Delta t = 50\ \mu$s. In all these calculations lasing is prevented by assuming $Q_0 = 1$.

sensing applications than the bulk case with freely diffusing dye molecules, due to the high sensitivity of the FRET rate to the molecular arrangement of the donor and acceptor molecules. In this section, we consider an optofluidic dye laser with a composite gain medium consisting of molecularly linked FRET pair dyes and simulate its lasing properties in order to understand its biosensing potential.

First, we carry out a benchmark analysis that establishes the sensitivity of a simple FRET-based biosensor operated in the absence of lasing, using solely spontaneous fluorescence emission as the measurement signal. Fig. 8 shows the results of such an analysis performed using our model, assuming [D–A] $= 5\ \mu$M and a very low Q-factor of the laser cavity ($Q_0 = 1$) to ensure that lasing is prevented. In Fig. 8(a) and (b), we present the donor and acceptor output energies E_{Dout} and E_{Aout} as a function of R for different values of Φ_P at two different excitation pulsewidths, $\Delta t = 5$ ns and $\Delta t = 50\ \mu$s, respectively. In order to quantify the changes in the donor or acceptor emission energies E_{Dout}, E_{Aout} triggered by changing the value of a physical parameter X, we define sensitivity, $\Omega(X)$, of emission energy to this parameter using $\Omega(X) = |(100 \times dE_{\text{out}})/(E_{\text{out}} dX)|$. In Fig. 8(c) and (d), the donor emission sensitivity ($\Omega_D(R) = |(100 \times dE_{\text{Dout}})/(E_{\text{Dout}} dR)|$) is plotted as a function of R for a non-lasing linked donor/acceptor dye pair at different values of Φ_P for $\Delta t = 5$ ns and $\Delta t = 50\ \mu$s, respectively. Similarly, Fig. 8(e) and (f) shows the acceptor emission sensitivity ($\Omega_A(R) = |(100 \times dE_{\text{Aout}})/(E_{\text{Aout}} dR)|$) as a function of R for a non-lasing linked donor/acceptor dye pair at different values of Φ_P for $\Delta t = 5$ ns and $\Delta t = 50\ \mu$s, respectively.

As illustrated by Fig. 8(c) and (e), when Φ_P increases, Ω_D decays faster with increasing R and the maximum of Ω_A shifts toward smaller R values. This behavior is mainly due to the saturation in the absorption of donor molecules. In the absence of the acceptor, output energy of fluorescence emission from the donor dye molecules excited with low pump power depends linearly on the pump power. However, with increasing pump power, output energy of the donor eventually saturates as the number of available dye molecules in the ground state decreases because of the limited decay rate of the donor excited state. In the presence of the acceptor, FRET serves as an additional depletion channel for the excited donor molecules, enabling their faster decay to the ground state and mitigating the effect of saturation. At low pump power when $N_d \gg n_d$, donor absorption represented by the first term on the right-hand side of Eq. (1) is virtually independent of R. Hence, the dependence of Ω_D and Ω_A on R derives solely from the changes in FRET efficiency given by Eq. (9). However, when the pump power, which is directly proportional to $\Phi_P/\Delta t$, approaches the saturation value of donor absorption, n_d becomes comparable to N_d and, consequently, donor absorption becomes a function of R. Thus, the profiles of $\Omega_D(R)$ and $\Omega_A(R)$ are now determined by the interplay between simultaneously changing FRET efficiency and donor absorption. As the pump power increases toward donor saturation, more assistance from FRET is needed to bring the donor molecules back to the ground state where they can absorb again the pump photons. This leads to a faster decay of Ω_D with increasing R and shifting of maximal values of Ω_A to smaller R where FRET is more efficient.

In order to quantify the donor and acceptor emission sensitivities in a conventional FRET-based bio-sensing assay which typically uses low-power continuous-wave excitation, we carry out simulations with the pump pulsewidth increased from $\Delta t = 5$ ns to $\Delta t = 50\ \mu$s. For a constant pump fluence, this translates to the decrease of the average pump power by four orders of magnitude, which means the system operates well below the donor saturation level. Consequently, the profiles of $\Omega_D(R)$ and $\Omega_A(R)$ are independent of the value of Φ_P, following directly the FRET efficiency changes described by Eq. (9) [see Fig. 8(d) and (f)]. In the following, we will use these pump power-invariant linker length sensitivities as a benchmark in comparing and quantifying the performance of biosensors based on optofluidic FRET lasers.

Next, in Fig. 9, we consider FRET lasing in a high-Q ($Q_0 = 10^6$) cavity and quantify the improvements in sensitivity that can be achieved assuming a linked donor/acceptor pair with [D–A] $= 5\ \mu$M, the same concentration as considered in Fig. 8. Fig. 9(a) and (b) shows the total output energy emitted from the donor and acceptor molecules versus Φ_P for different R values. In Fig. 9(a), the donor lasing threshold decreases with increasing linker length because of the lower energy transfer to the acceptor and, thus, lower loss. In contrast, increasing

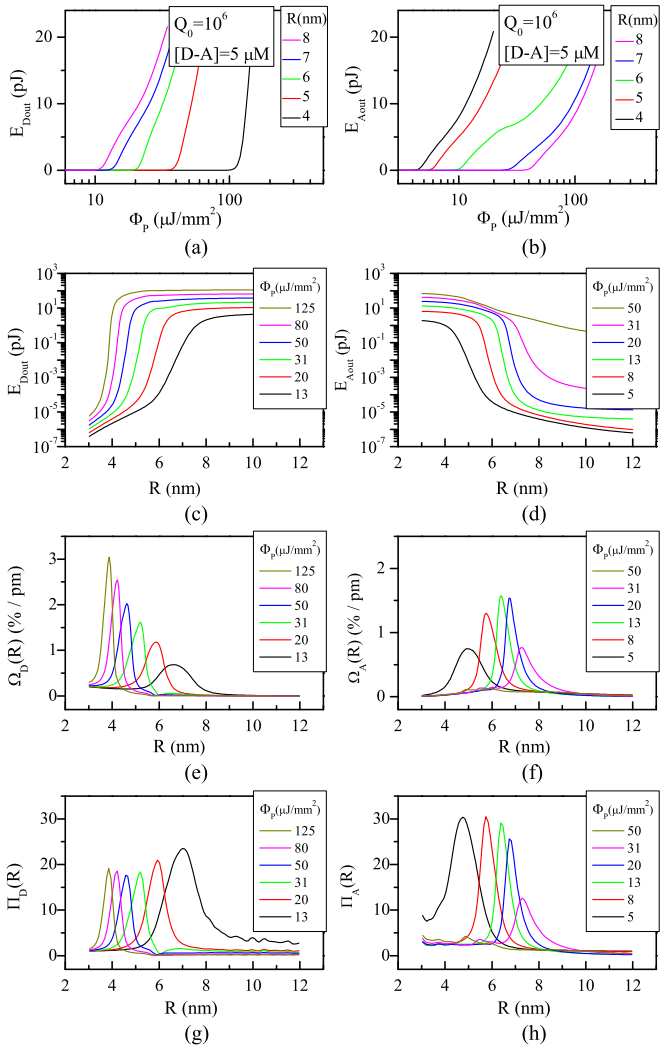

Fig. 9. Behavior of FRET lasing-based biosensor for changing linker length R. Total output energy of (a) donor and (b) acceptor versus Φ_P for different values of R. Total output energy of (c) donor and (d) acceptor versus R for different values of Φ_P. The linker length sensitivity for (e) donor, $\Omega_D(R)$, versus R and (f) acceptor, $\Omega_A(R)$, versus R, calculated for FRET lasing emission from linked donor/acceptor pairs at different values of Φ_P and a constant value of donor/acceptor complex concentration, $[\mathrm{D{-}A}] = 5\ \mu\mathrm{M}$. The sensitivity enhancement factor for (g) donor and (h) acceptor as a function of linker length at different Φ_P values. In all simulations, excitation pulse width was set to $\Delta t = 5$ ns and the cavity Q-factor was 10^6.

linker length leads to increasing lasing threshold for the acceptor as the pumping efficiency becomes lower due to reduction in FRET rate [see Fig. 9(b)]. In Fig. 9(c) and (d), we present the dependence of E_{Dout} and E_{Aout}, on R at different values of Φ_P. As expected from the above reasoning, at all studied values of Φ_P, E_{Dout} increases monotonously with R whereas E_{Aout} displays the opposite trend.

Fig. 9(e) and (f) show $\Omega_D(R)$ and $\Omega_A(R)$ as a function of R at different values of Φ_P. For all values of Φ_P, the profiles of $\Omega_D(R)$ and $\Omega_A(R)$ have Lorentzian-like shapes. With increasing Φ_P, the peak value of $\Omega_D(R)$ increases monotonously and the position of the peak moves toward lower values of R. In contrast, the peak value of $\Omega_A(R)$ reaches maximum for a specific Φ_P which lies around 13 $\mu\mathrm{J/mm}^2$ for the studied Q-factor and FRET complex concentration [D–A]. At the same time, peak position of $\Omega_A(R)$ moves toward higher R for increasing Φ_P. The fact that the acceptor sensitivity to the linker length $\Omega_A(R)$ reaches maximum at an intermediate pump fluence Φ_P stems from the combined effect of FRET and CET on the acceptor lasing and it is studied in detail in the next section.

To quantify the enhancement in sensitivity achieved by biosensors based on optofluidic FRET laser as compared to a biosensor using non-lasing FRET, we define the sensitivity enhancement factor Π as the ratio of lasing FRET sensitivity to the regular fluorescence FRET sensitivity, $\Pi = \Omega_{\mathrm{lasing}}(X)/\Omega_{\mathrm{fluorescence}}(X)$. Here, $\Omega_{\mathrm{lasing}}(X)$ is the sensitivity of the output energy of stimulated emission from the donor or acceptor placed inside a high-Q cavity to changes in parameter X characterizing the gain medium whereas $\Omega_{\mathrm{fluorescence}}(X)$ is the corresponding sensitivity of the output energy of regular (non-amplified) fluorescence from the donor or acceptor placed inside a cavity with $Q_0 = 1$. Parameter X can be either the donor/acceptor distance R (representing conformational changes in linked dye complex) or the dye complex concentration [D–A]. Fig. 9(g) and (h) shows $\Pi_D(R)$ and $\Pi_A(R)$, the donor and acceptor sensitivity enhancement factors, versus R, respectively. In order to calculate $\Pi_D(R)$ and $\Pi_A(R)$, the values of Ω_{lasing} were taken from Fig. 9(e) and (f), respectively, whereas the corresponding benchmark values of $\Omega_{\mathrm{fluorescence}}$ come from Fig. 8(d) and (f), respectively. As illustrated by Fig. 9(g) and (h), maximal enhancement factors of $\sim$20 for donor and $\sim$25 for acceptor sensitivities are observed for a relatively broad range of R at low pump fluences Φ_P. According to Fig. 9(g), the value of $\Pi_D(R)$ reaches maximum for the minimal studied pump fluence $\Phi_P = 13\ \mu\mathrm{J/mm}^2$ and then decreases with increasing Φ_P whereas $\Omega_D(R)$ displays the opposite trend [see Fig. 9(e)]. This behavior can be explained by the saturation of donor absorption at high pump fluences which was discussed in detail in Fig. 8. In particular, the absorption of lasing donor pumped with $\Delta t = 5$ ns pulses at $\Phi_P > 13\ \mu\mathrm{J/mm}^2$ becomes partially saturated which in turn reduces the effective value of $\Omega_{D,\mathrm{lasing}}(R)$. At the same time, saturation is completely avoided in the benchmark values of $\Omega_{D,\mathrm{fluorescence}}(R)$ which are calculated assuming long pump pulses with $\Delta t = 50\ \mu$s. As a result, $\Pi_D(R) = \Omega_{D,\mathrm{lasing}}(R)/\Omega_{D,\mathrm{fluorescence}}(R)$ is reduced. By lowering Φ_P, the saturation effects are also suppressed in the lasing case and, consequently, the enhancement factor $\Pi_D(R)$ increases. For the case of acceptor, the reason of reduction in $\Pi_A(R)$ for $\Phi_P > 8\ \mu\mathrm{J/mm}^2$ is the progressively increasing magnitude of CET which reduces the sensitivity of the acceptor output energy to the linker length R. For the studied dye complex concentration $[\mathrm{D{-}A}] = 5\ \mu\mathrm{M}$, minimal donor lasing threshold corresponding to $R \gg R_0$ is $\Phi_P \approx 13\ \mu\mathrm{J/mm}^2$; upon crossing this value of Φ_P, donor lasing is triggered. Consequently, CET increases dramatically which leads to a drop in $\Pi_A(R)$.

V. Effect of Q-Factor on $\Omega_D(R)$ and $\Omega_A(R)$ in Linked FRET Pair Biocomplexes

As mentioned briefly in the previous section, sensitivity of the acceptor lasing emission to the linker length $\Omega_A(R)$ is determined by the combined effect of FRET and CET; relative importance of these two mechanisms of acceptor pumping depends

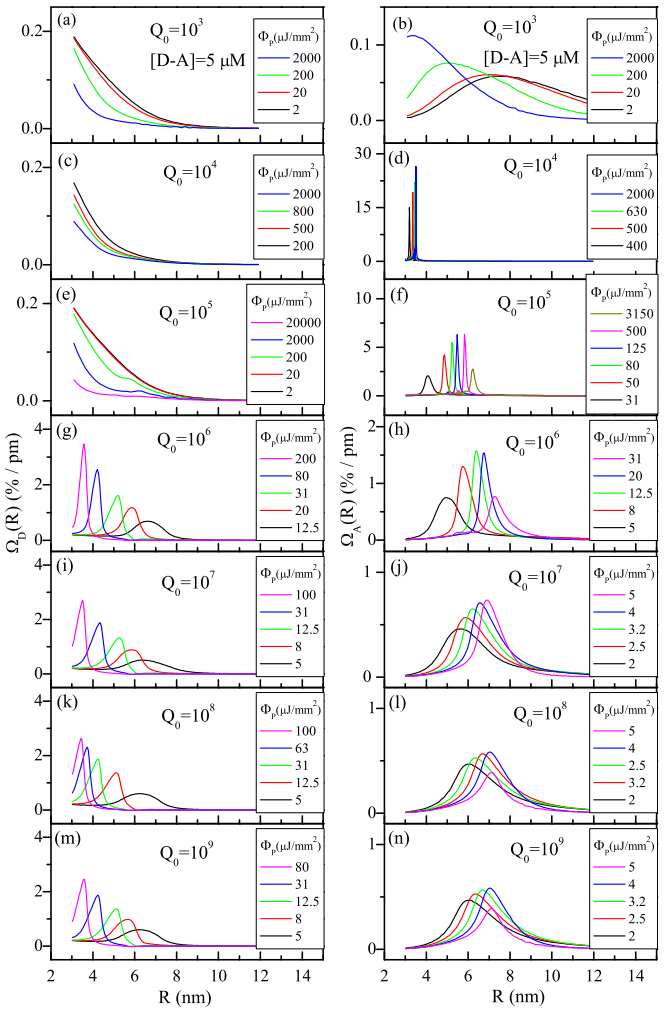

Fig. 10. Effect of the cavity Q-factor on emission sensitivities of donor, $\Omega_D(R)$, and acceptor, $\Omega_A(R)$, for linked 1D−1A donor/acceptor complexes at different values of Φ_P and a fixed concentration, $[\mathrm{D{-}A}] = 5\ \mu\mathrm{M}$. In (a), (c) and (e) for donor and in (b) for acceptor no lasing is observed.

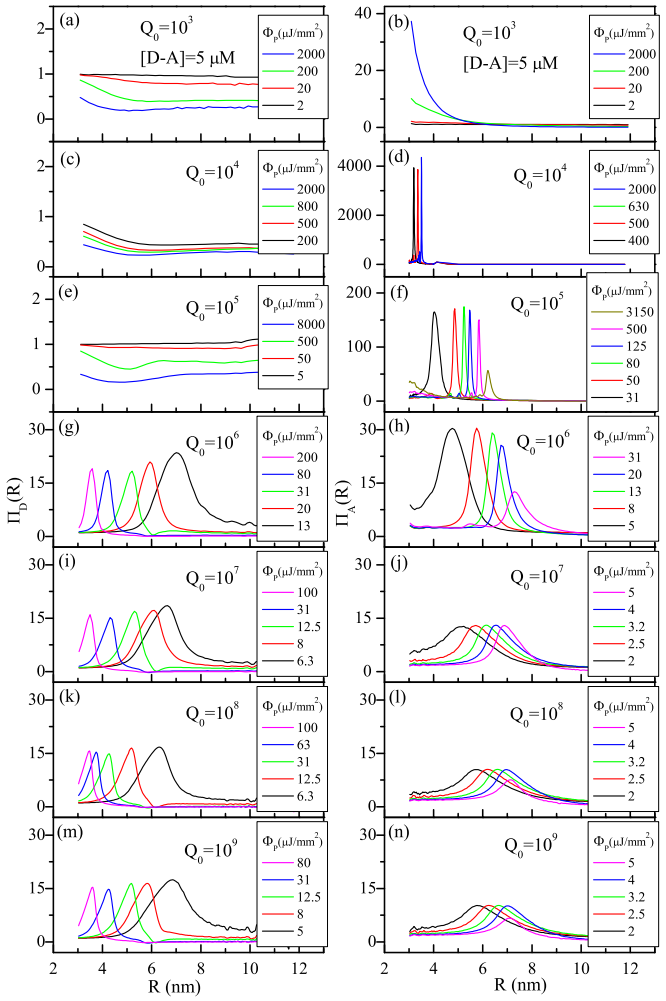

Fig. 11. Effect of the cavity Q-factor on sensitivity enhancement factors for donor, $\Pi_D(R)$, and acceptor $\Pi_A(R)$ versus R in linked 1D−1A donor/acceptor complexes at different values of Φ_P and a fixed complex concentration of $[\mathrm{D{-}A}] = 5\ \mu\mathrm{M}$.

on the cavity Q-factor. In this section, we study the influence of Q-factor in a more systematic way. Fig. 10 shows emission sensitivities Ω_D and Ω_A for different cavity Q-factors ranging between 10^3–10^9 considering a constant $[\mathrm{D{-}A}] = 5\ \mu\mathrm{M}$. For each Q-factor, excitation conditions were fine-tuned in order to reveal Φ_P necessary for achieving the maximum FRET sensitivities in donor and acceptor that occur around their respective lasing thresholds. For the case of $Q_0 = 10^3, 10^4$ and 10^5 for donor [see Fig. 10(a), (c), and (e)] and for $Q_0 = 10^3$ for acceptor [see Fig. 10(b)], no lasing is observed even at very high Φ_P values. Hence, in these cases, the lasing FRET sensitivity curves are similar to the case of fluorescence FRET sensitivities shown in Fig. 8(c) and (e). Fig. 11 shows the sensitivity enhancement factors, Π_D and Π_A, obtained for cases considered in Fig. 10 using the non-amplified spontaneous FRET sensitivities of Fig. 8(d) and (f) as the reference. In Fig. 11(a), (c), and (e), we see less than unity enhancement factor for donor molecules, $\Pi_D \lesssim 1$, in the range of R under study. In contrast, for acceptor molecules, in Fig. 11(b), (d), and (f), we see relatively large enhancement factors. In particular, Π_A takes values of more than 30, 4000, and 150 in Fig. 11(b), (d), and (f), respectively. In Fig. 11(a) and (b), Π_D and Π_A largely deviate from unity, especially at high Φ_P values, despite the absence of both donor and acceptor lasing emissions. This is due to the saturation in donor absorption that effects $\Omega_D(R)$ and $\Omega_A(R)$ curves at high Φ_P values, as we previously explained for Fig. 8(c) and (e). However, we should note that the high Π_A values in Fig. 11(b) do not represent higher absolute sensitivities Ω_A. As we can see in Fig. 10(b), for different values of Φ_P values, the maximum value of Ω_A is around 0.05–0.1%/pm, only the value of R corresponding to the maximum of Ω_A is observed to change. Among the relatively low Q-factor cases ($Q_0 = 10^3$, 10^4, and 10^5), the results obtained for $Q_0 = 10^5$ are especially noteworthy because for this case, high enhancement of more than 150 is achieved for a broad range of R values around R_0, the most interesting range of distances used in typical FRET-based biosensor experiments.

For Q-factors larger than 10^6, donor lasing is observed together with acceptor lasing. As a result, Π_D reaches peak values between 15–20 for Q-factors ranging between 10^6–10^9. With the emergence of donor lasing, a drop is observed in the peak values of Π_A. The peak value of Π_A which is more than 150

for $Q_0 = 10^5$ decreases to around 30 for $Q_0 = 10^6$, as a result of the onset of donor lasing. As Q_0 is further increased from 10^6 in Fig. 11(h) up to 10^9 in Fig. 11(n), the peak value of Π_A gradually drops from 30 to around 8. This additional drop of the acceptor sensitivity enhancement with increased Q-factor can be attributed to the growing importance of CET, which is insensitive to the donor–acceptor distance, and its eventual dominance over FRET in higher Q-factors. To evaluate the role of CET in the sensitivity reduction at high Q-factors, we use the approach that has been developed by Folan *et al.* [27] for the evaluation of CET effect evaluation in aerosol droplets and that is also applicable to other cavities [25]. In this approach CET is assumed to happen in two steps. In the first step, photons from the donor emission couple to the modes of the resonator with the highest Q-factors. Subsequently, those resonant photons are absorbed by the acceptor chromophores. The CET probability which is the probability of a photon emitted from donor to be absorbed by acceptor molecules with concentration of ρ_a, can be calculated using [25]:

$$P = \frac{\sigma_{aad}\rho_a c/\eta}{1/\tau_{cd} + \sigma_{aad}\rho_a c/\eta}. \tag{10}$$

According to this equation, for $1/\tau_{cd} \gg \sigma_{aad}\rho_a c/\eta$, P is a function of acceptor concentration but for $1/\tau_{cd} \ll \sigma_{aad}\rho_a c/\eta$ which corresponds to a high-Q cavity, P becomes equal to one. The characteristic acceptor concentration at which the full radiative cavity-assisted energy transfer falls by a factor of 2 ($\rho_{a1/2}$) can be determined by $\rho_{a1/2} = \eta/(\tau_{cd}\sigma_{aad}c)$. Using the numerical values from Table I, we find $\rho_{a1/2}$ =160 and 16 μM, for quality factors of $Q_0 = 10^5$ and 10^6, respectively. Hence, for 1D–1A complex structure with $[\mathrm{D\text{–}A}] = 5$ μM, we expect the CET probabilities to be 3% and 30%, respectively, for $Q_0 = 10^5$ and 10^6. CET probability is independent of R; hence, when it becomes comparable to or bigger than FRET rate, a dramatic decrease is observed in the R sensitivity of the donor and acceptor lasing emissions. This explains the decrease in the maximum values of Π_D and Π_A with increase in Q-factor from 10^6 to 10^9 in Fig. 11. Besides, having a minimum necessary Q-factor to enable acceptor lasing but not donor lasing (as observed for $Q_0 = 10^4$ in Fig. 11(c) and (d)) results in a giant jump in the acceptor emission sensitivity. Hence, as a rule of thumb, for a given cavity with a fixed Q-factor, in order to achieve the highest possible sensitivities using optofluidic FRET lasers, CET should be suppressed by choosing sufficiently small acceptor concentrations, i.e., $\rho_a \ll \rho_{a1/2}$.

The total Q-factor Q_0 of the resonator can be found as $Q_0^{-1} = Q_s^{-1} + Q_r^{-1}$ where $Q_s = 2\pi\eta/(\lambda\alpha_s)$ is due to the absorptive losses in a medium with absorption coefficient α_s and $Q_r = 2\pi l/[\lambda(1-\mathcal{R})]$ is due to the radiative out-coupling by identical cavity mirrors with reflectance $\mathcal{R}$ [28]. For the laser gain medium formed by an aqueous solution of donor and acceptor dyes, the absorption coefficient of water at the donor lasing wavelength is $\alpha_s(\lambda_d) \approx 6 \times 10^{-4}$ cm^{-1} which is six times lower than the corresponding value at the acceptor lasing wavelength $\alpha_s(\lambda_a) \approx 35 \times 10^{-4}$ cm^{-1} [29]. Assuming $\mathcal{R} \to 1$ and using water absorption coefficients at the donor and acceptor lasing wavelengths, the corresponding maximal absorption-limited Q-factors are $Q_0(\lambda_d) = 2.5 \times 10^8$ and $Q_0(\lambda_a) = 3.6 \times 10^7$, respectively. Taking this into account, we can conclude that the absorption of water has no effect on the curves of $\Omega(R)$ and $\Pi(R)$ calculated for $Q_0 \leq 10^7$. However, for Q_0 lying between 10^7 and the respective absorption-limited maximal Q-factor values at λ_d and λ_a, the realistic curves of $\Omega(R)$ and $\Pi(R)$ would be slightly different from those presented in Figs. 10 and 11.

VI. Sensitivity of Detection for Conformational Changes in 1D–3A and 3D–1A Biocomplexes

When the donor and acceptor dye molecules are connected to each other using a suitable nanometer-scale rigid linker (for example, a DNA fragment or a polypeptide), in addition to the separation distance between the dyes, the donor-to-acceptor ratio can be pre-determined in each dye complex. This opens up new possibilities for tuning of the laser gain in FRET-based optofluidic lasers [13]. Naturally, such control of the donor/acceptor stoichiometry can also be beneficial in sensing applications. To evaluate the performance of FRET lasing-based biosensors with variable donor-to-acceptor ratio, we study two different linked dye complexes which are schematically illustrated in Fig. 1(c). In the first one, we assume a single donor molecule attached by three identical linkers to three acceptor molecules (1D–3A) whereas in the second one, there are three donor molecules linked to a single acceptor molecule by identical linkers (3D–1A). Figs. 12 and 13 show the total output energy versus Φ_P and also the total output energy, Ω_D, Ω_A, Π_D and Π_A, versus R, for 1D–3A and 3D–1A complexes, respectively, for a cavity with $Q_0 = 10^6$. In both studied complexes, the concentration of acceptor is fixed at $[\mathrm{A}] = 9$ μM. Consequently, overall concentration of the dye complex is 3 μM for 1D–3A and 9 μM for 3D–1A. Accordingly, the donor concentration is 3 μM in case of 1D–3A and 27 μM in case of 3D–1A. Comparison of Figs. 12(b) and 13(b) show that for the values of R varying between 4–8 nm, the acceptor lasing threshold of 3D–1A complex is seven to nine times lower than the corresponding threshold of 1D–3A complex. This is because of more efficient pumping from the donor side in 3D–1A complexes in comparison with 1D–3A complexes since there are more donors in 3D–1A complexes. This finding is in agreement with our previous experimental results obtained with donor/acceptor complexes linked by tetrahedral DNA scaffold structures and also with theoretical predictions based on an approximate analytical method of lasing threshold estimation [10], [30], [31].

Evaluation of lasing FRET sensitivity curves for donor, Ω_D, and acceptor, Ω_A [see Figs. 12(e), (f) and 13(e), (f)] and their corresponding spontaneous fluorescence FRET sensitivity curves which are not shown here, results in enhancement factors Π_D and Π_A shown in Figs. 12(g), (h) and 13(g), (h). Here, the maximal enhancements Π_D and Π_A for 1D–3A are around 15 and 30, respectively, while they are both around 30 in 3D–1A. Hence, in 3D–1A, twofold enhancement is observed in donor sensitivity as compared to 1D–3A case, while acceptor sensitivities are comparable in both linked dye complexes. This is because of the CET rate dominance over FRET rate at this acceptor concentration.

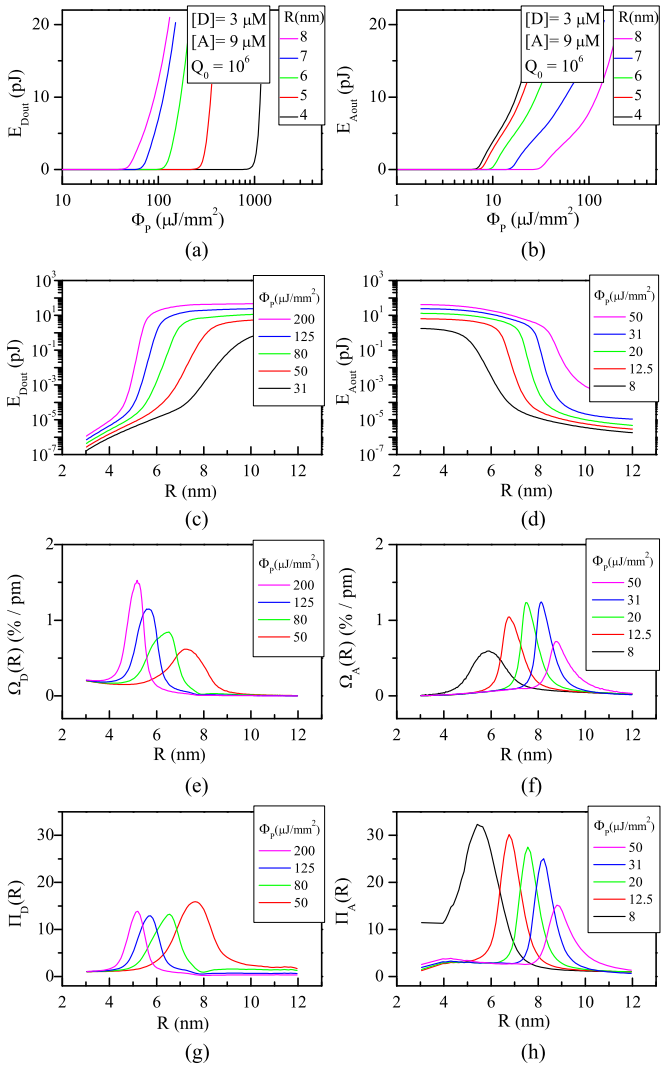

Fig. 12. Behavior of FRET lasing-based biosensor using 1D–3A linked dye complexes with changing R. Total output energy of (a) donor and (b) acceptor versus Φ_P for different values of R. Total output energy of (c) donor and (d) acceptor versus R for different values of Φ_P. The emission sensitivity for (e) donor, $\Omega_D(R)$, and (f) acceptor $\Omega_A(R)$, versus R calculated for FRET lasing emission from linked donor/acceptor complexes at different values of Φ_P. Sensitivity enhancement factors for (g) donor, $\Pi_D(R)$, and (h) acceptor $\Pi_A(R)$, versus R calculated for linked donor/acceptor complexes at different values of Φ_P. In all calculations, 1D–3A linked dye complexes are assumed to have equal link distances between the donor and acceptor molecules. Effective donor concentration is $[\mathrm{D}] = 3\ \mu\mathrm{M}$, effective acceptor concentration is $[\mathrm{A}] = 9\ \mu\mathrm{M}$.

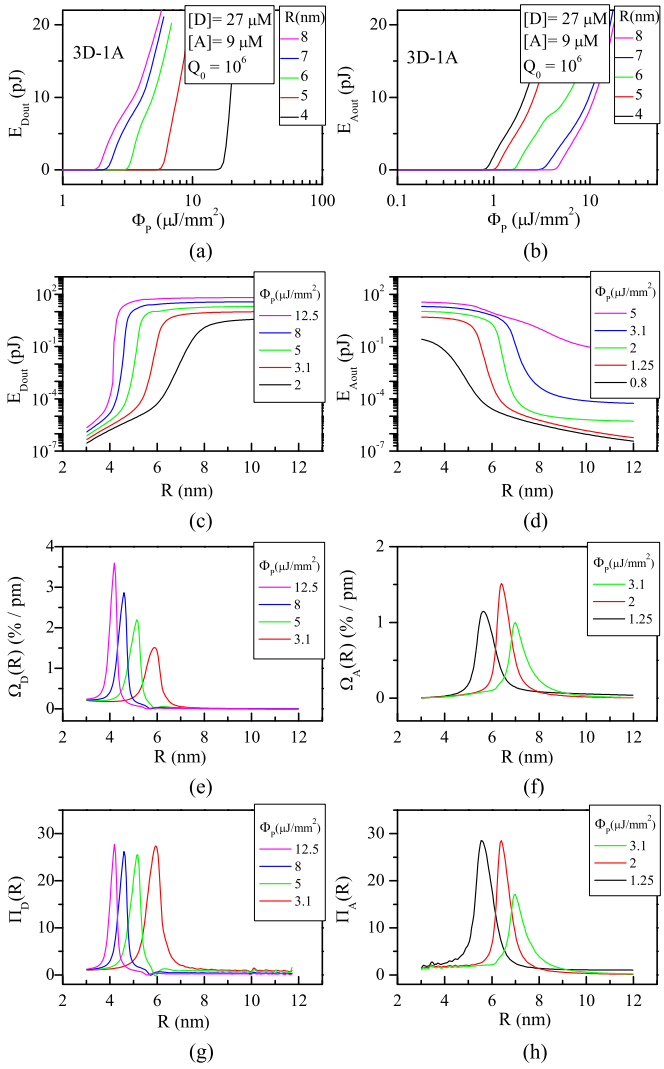

Fig. 13. Behavior of FRET lasing-based biosensor using 3D–1A linked dye complexes with changing R. Total output energy of (a) donor and (b) acceptor versus Φ_P for different values of R. Total output energy of (c) donor and (d) acceptor versus R for different values of Φ_P. The emission sensitivity for (e) donor, $\Omega_D(R)$ and (f) acceptor, $\Omega_A(R)$, versus R calculated for FRET lasing emission from linked donor/acceptor complexes at different values of Φ_P. Sensitivity enhancement factors for (g) donor, $\Pi_D(R)$, and (h) acceptor $\Pi_A(R)$, versus R calculated for linked donor/acceptor complexes at different values of Φ_P. In all calculations, 3D–1A linked dye complexes are assumed to have equal link distances between the acceptor and donor molecules. Effective donor concentration is $[\mathrm{D}] = 27\ \mu\mathrm{M}$, effective acceptor concentration is $[\mathrm{A}] = 9\ \mu\mathrm{M}$.

To increase the enhancement factor even further, the total concentration of the acceptor in the $Q_0 = 10^6$ cavity can be decreased to less than $\sim 1.6\ \mu$M. This value is calculated as $\rho_{a1/2}/10$, based on the rule of thumb ($\rho_a \ll \rho_{a1/2}$) discussed in the previous section. In such small concentrations, the presence of three donor molecules per single acceptor molecule in 3D–1A compared to one donor in 1D–1A and 1/3 donor in 1D–3A, will help the acceptor molecules in 3D–1A to be pumped more efficiently in comparison to 1D–1A and 1D–3A. This in turn allows using lower values of Φ_P and, thus, extending the lifetime of the biochemical sensor by decreasing the risk of chromophore photobleaching.

VII. Concentration Sensitivity in FRET Lasing-Based Biosensors

In addition to analyzing the donor/acceptor sensitivity, Ω_D and Ω_A, to changes in R, it is interesting to study the sensitivity to changes in the complex concentration [D–A], defined by $\Omega_D([D\text{–}A]) = |(100 \times dE_{\mathrm{Dout}})/(E_{\mathrm{Dout}} d[D\text{–}A])|$ and $\Omega_A([D\text{–}A]) = |(100 \times dE_{\mathrm{Aout}})/(E_{\mathrm{Aout}} d[D\text{–}A])|$ for donor and acceptor, respectively. This situation mimics a biosensing scenario in which FRET dye pairs are removed from or added to the gain medium due to an underlying biological process such as ligand-receptor binding and unbinding. The results of

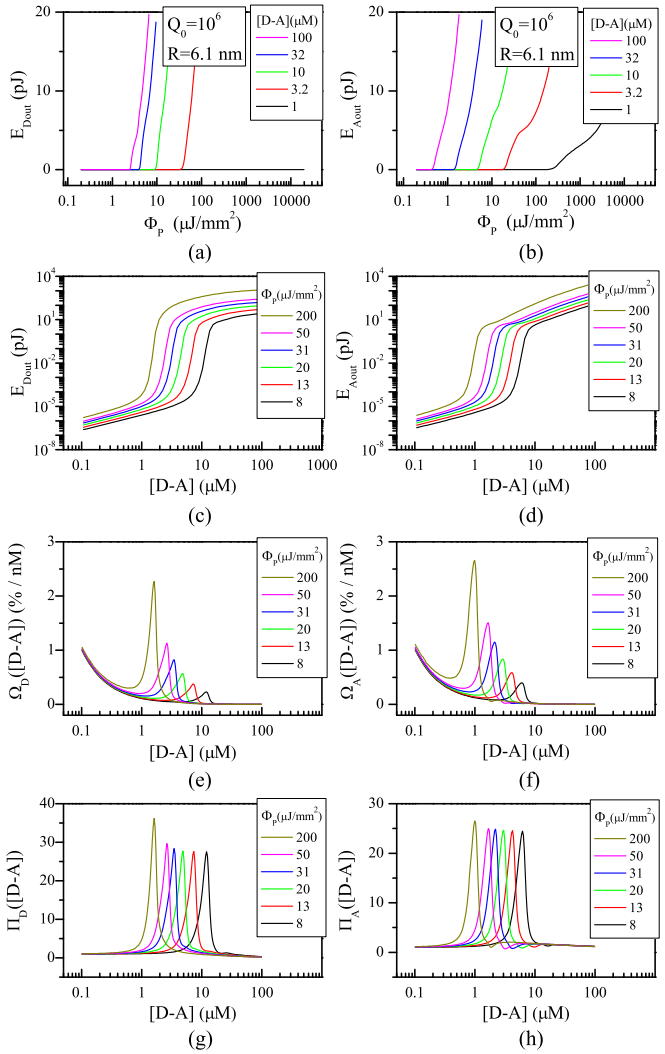

Fig. 14. Behavior of FRET lasing-based biosensor with changing concentration of linked complex [D–A]. Total output energy of (a) donor and (b) acceptor versus Φ_P for different values of [D–A]. Total output energy of (c) donor and (d) acceptor versus [D–A] for different values of Φ_P. The complex concentration sensitivity of (e) donor and (f) acceptor versus [D–A] calculated for FRET lasing emission from linked donor/acceptor pairs at different values of Φ_P. The complex concentration sensitivity enhancement factor for (g) donor and (h) acceptor versus [D–A] for FRET lasing emission from linked donor/acceptor pairs at different values of Φ_P. In all calculations, R is assumed to be equal to R_0.

such concentration-dependent study are summarized in Fig. 14 which shows the total output energy from the donor and acceptor as a function of Φ_P (parts (a) and (b)) and FRET complex concentration [D–A] (parts (c) and (d)). In all simulations, cavity Q-factor is fixed at 10^6 and the donor–acceptor distance is set to $R = R_0 = 6.1$ nm. The dependence of $\Omega_D([D\text{–}A])$ and $\Omega_A([D\text{–}A])$ on [D–A] for different values of Φ_P, assuming a constant $R = R_0$, is then summarized in Fig. 14(e) and (f) for donor and acceptor, respectively. As illustrated in Fig. 14(e) and (f), the maximum sensitivity values are reached at lower concentrations [D–A]. This is due to a larger relative change in the lasing pair population by addition or subtraction of individual FRET pairs when [D–A] is smaller. Hence, achieving FRET lasing with minimal FRET pair concentration is critical for maximizing the concentration sensitivity. Here, our calculations

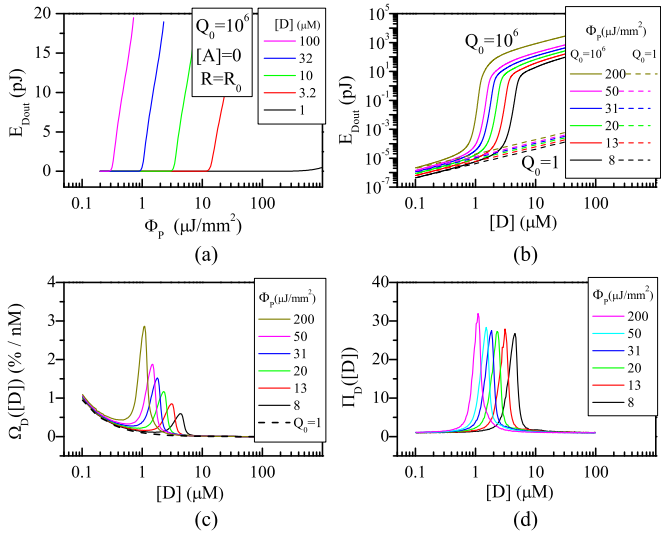

Fig. 15. Behavior of a single dye laser for changing concentration of the gain medium [D]. (a) Total output energy from a single dye, R6G, for $Q_0 = 10^6$ versus Φ_P for different values of [D], (b) Total output energy from a single dye, R6G, for $Q_0 = 10^6$ with solid lines and for $Q_0 = 1$ with dashed lines versus [D] for different values of Φ_P. (c) Concentration sensitivity of emission from a single dye for $Q_0 = 10^6$ with solid lines and for $Q_0 = 1$ with dashed line versus [D] at different values of Φ_P. (d) Concentration sensitivity enhancement factor for single dye versus [D] relative to the nonlasing emission at different values of Φ_P.

show that for $\Phi_P = 200\ \mu\text{J/mm}^2$, remarkable [D–A] concentration sensitivities that are larger than $2\%/\text{nM}$ and $2.5\%/\text{nM}$ can be achieved for donor and acceptor emission, respectively [see Fig. 14(e) and (f)]. As in the studies of the linker length sensitivity, sensitivity enhancement factors for donor and acceptor, $\Pi_D([D\text{–}A])$ and $\Pi_A([D\text{–}A])$ are found by dividing the lasing FRET sensitivity with the fluorescence FRET sensitivity and displayed in Fig. 14(g) and (h), versus [D–A]. Depending on the values of Φ_P, maximal sensitivity enhancement are observed at different complex concentrations but their peak values in a wide range of [D–A], from 1 to 10 μM have approximately constant values around 25 that show a 25-times improvement relative to non-lasing FRET sensing. To evaluate the concentration sensitivity for single dye lasing, in Fig. 15, we perform the analysis similar to that shown in Fig. 14, but just for donor molecules without any acceptors. As shown in Fig. 15(a), donor lasing threshold in the absence of acceptor is lower relative to that of FRET lasing shown Fig. 14(a) which is caused by depletion of the donor excited state by FRET in the latter case. In Fig. 15(b), the total output energies for $Q_0 = 10^6$ and $Q_0 = 1$ are shown, respectively, by solid and dashed lines versus [D]. In Fig. 15(c), $\Omega_D([D])$ is shown versus [D] at different values of Φ_P assuming $Q_0 = 10^6$ with solid lines and $Q_0 = 1$ with the dashed line. For the case of spontaneous fluorescence emission ($Q_0 = 1$, i.e., no lasing), concentration sensitivity is independent of the value of Φ_P. In Fig. 15(d), the enhancement factor of concentration sensitivity relative to the spontaneous fluorescence measurements shows higher than 25-fold improvement in the maximal sensitivity. In both Figs. 15(d) and 14(g), the minimum sensible donor or donor/acceptor complex

concentration at which sensitivity enhancement due to lasing can be achieved is limited to about 1 μM. However, by using emission of linked acceptor molecules and by choosing linker lengths smaller than R_0, concentration sensitivity enhancement can be reached at even lower concentrations down to 0.1 μM. This can be understood from the linked donor/acceptor threshold curves shown in Fig. 6(b). For $R = 3$ nm, acceptor can lase down to 0.1 μM which means an order of magnitude expansion toward the nanomolar concentration region.

VIII. Conclusion

We have presented a comprehensive theoretical analysis of optofluidic lasers with composite active media formed by a pair of donor and acceptor dyes which can participate in radiative and non-radiative (FRET) energy transfer pathways within the laser cavity. We draw the following main conclusions from our analysis:

- Parametric study of the conceptually distinct cases of energy transfer between donor and acceptor molecules diffusing freely in bulk solution and molecules connected by a fixed-length linker showed that the latter arrangement with concentration-independent FRET rate is especially well suited for FRET-based sensing of low-concentration analytes.
- In comparison to conventional FRET sensors using spontaneous fluorescence emission, biochemical sensors based on FRET lasing from linked donor–acceptor complexes can bring about more than 100-fold enhancement of detection sensitivity of conformation changes of the complex for linker lengths comparable to the Förster radius of the donor–acceptor pair. Such high sensitivities can be achieved by choosing the pump fluence near the lasing threshold of the donor or acceptor molecules for a given dye pair concentration.
- Higher Q-factor of the laser cavity does not necessarily result in higher sensitivity to conformational changes in a FRET lasing-based biochemical sensor. At very high Q factors, radiative energy transfer dominates over FRET, thus hampering the performance of FRET laser-based biochemical sensor. Our analysis has revealed that cavities with Q-factors between 10^4–10^6 enable optimal sensing performance.
- Biochemical sensors based on FRET lasing from linked donor-acceptor complexes can provide more than 20-fold enhancement in the sensitivity of FRET signals to dye-pair concentration by choosing an optimal pump fluence and concentration range of the linked complex. Under such experimental conditions, more than 1% change can be observed in donor or acceptor emission intensities for 1 nM change in dye-pair concentration of approximately 1 μM.

Our theoretical findings which are supported by experimental results reported recently in the literature provide a basic set of tools for design and optimization of novel FRET-based biosensors and tunable integrated sources of coherent light.

Acknowledgment

The author would like to thank E. Özelci for fruitful discussions on the development of the rate equation model.

References

[1] S. Zadran *et al.*, "Fluorescence resonance energy transfer (FRET)-based biosensors: Visualizing cellular dynamics and bioenergetics," *Appl. Microbiol. Biotechnol.*, vol. 96, no. 4, pp. 895–902, Nov. 2012.

[2] I. T. Li, E. Pham, and K. Truong, "Protein biosensors based on the principle of fluorescence resonance energy transfer for monitoring cellular dynamics," *Biotechnol. Lett.*, vol. 28, no. 24, pp. 1971–1982, Nov. 2006.

[3] S. I. Shopova *et al.*, "Opto-fluidic ring resonator lasers based on highly efficient resonant energy transfer," *Opt. Exp.*, vol. 15, no. 20, pp. 12 735–12 742, 2007.

[4] M. Berggren, A. Dodabalapur, R. E. Slusher, and Z. Bao, "Light amplification in organic thin films using cascade energy transfer," *Nature.*, vol. 389, no. 6650, pp. 466–469, Oct. 1997.

[5] Z. Li and D. Psaltis, "Optofluidic dye lasers," *Microfluid. Nanofluid.*, vol. 4, nos. 1/2, pp. 145–158, Jan. 2008.

[6] X. Fan and I. M. White, "Optofluidic microsystems for chemical and biological analysis," *Nature Photon.*, vol. 5, no. 10, pp. 591–597, Sep. 2011.

[7] X. Fan and S. H. Yun, "The potential of optofluidic biolasers," *Nature Methods*, vol. 11, no. 2, pp. 141–147, Jan. 2014.

[8] Y. Sun and X. Fan, "Distinguishing DNA by analog-to-digital-like conversion by using optofluidic lasers," *Angew. Chem. Int. Ed.*, vol. 51, no. 5, pp. 1236–1239, Jan. 2012.

[9] X. Zhang, W. Lee, and X. Fan, "Bio-switchable optofluidic lasers based on DNA holliday junctions," *Lab Chip*, vol. 12, no. 19, pp. 3673–3675, 2012.

[10] Q. Chen *et al.*, "Highly sensitive fluorescent protein FRET detection using optofluidic lasers," *Lab Chip*, vol. 13, no. 14, pp. 2679–2681, 2013.

[11] W. Lee and X. Fan, "Intracavity DNA melting analysis with optofluidic lasers," *Anal. Chem*, vol. 84, no. 21, pp. 9558–9563, Oct. 2012.

[12] Y. Sun, S. I. Shopova, C.-S. Wu, S. Arnold, and X. Fan, "Bioinspired optofluidic fret lasers via DNA scaffolds," *PNAS* vol. 107, no. 37, pp. 16 039–16 042, 2010.

[13] Q. Chen *et al.*, "Self-assembled DNA tetrahedral optofluidic lasers with precise and tunable gain control," *Lab Chip*, vol. 13, no. 17, pp. 3351–3354, 2013.

[14] Q. Chen, M. Ritt, S. Sivaramakrishnan, X. Sun, and X. Fan, "Optofluidic lasers with a single molecular layer of gain," *Lab Chip*, vol. 14, no. 24, pp. 4590–4595, Oct. 2014.

[15] Z. S. Wang, H. A. Rabitz, and M. O. Scully, "The single-molecule dye laser," *Laser Phys.*, vol. 15, no. 1, pp. 118–123, 2005.

[16] J. Atkinson and F. Pace, "The spectral linewidth of a flashlamp-pumped dye laser," *IEEE J. Quantum Electron.*, vol. no. 9(6), pp. 569–574, Jun. 1973.

[17] J. Hebling, "20 ps pulse generation by an excimer laser pumped double self-Q-switched distributed feedback dye laser," *Appl. Phys. B.*, vol. 47, no. 3, pp. 267–272, Nov. 1988.

[18] J. Hebling, J. Seres, Z. Bor, and B. Racz, "Dye laser pulse shortening and stabilization by Q-switching," *Opt. Quantum Electron.*, vol. 22, no. 4, pp. 375–384, Jul. 1990.

[19] B. Ahamed and P. Palanisamy, "Nd:YAG laser pumped energy transfer distributed feedback dye laser in Rhodamine 6G and Acid blue 7 dye mixture," *Opt. Commun.*, vol. 213, pp. 67–80, Nov. 2002.

[20] Z. Bor and A. Muller, "Picosecond distributed feedback dye lasers," *IEEE J. Quantum Electron.*, vol. 22, no. 8, pp. 1524–1533, Aug. 1986.

[21] B. Valeur and M. Berberan-Santos, *Molecular Fluorescence: Principles and Applications*, 2nd ed. Weinheim, Germany: Wiley-VCH, Apr. 2012, ch. 9, pp. 247–273.

[22] T. Förster, "Experimentelle und theoretische untersuchung des zwischenmolekularen übergangs von elektronenanregungsenergie," *Z. Naturforsch. B*, vol. 4a, pp. 321–327, 1949.

[23] *The MathWorks, Inc.*, MATLAB R2011a, Natick, MA, USA, 2011.

[24] S. Arnold and L. M. Folan, "Energy transfer and the photon lifetime within an aerosol particle," *Opt. Lett.*, vol. 14, no. 8, pp. 387–389, Apr. 1989.

[25] P. T. Leung and K. Young, "Theory of enhanced energy transfer in an aerosol particle," *J. Chem. Phys.*, vol. 89, no. 5, pp. 2894–2899, 1988.
[26] S. Götzinger *et al.*, "Controlled photon transfer between two individual nanoemitters via shared high-Q modes of a microsphere resonator," *Nano Lett.*, vol. 6, no. 6, pp. 1151–1154, Jun. 2006.
[27] L. Folan, S. Arnold, and S. Druger, "Enhanced energy transfer within a microparticle," *Chem. Phys. Lett.*, vol. 118, no. 3, pp. 322–327, Jul. 1985.
[28] B. E. A. Saleh and M. C. Teich, *Fundamentals of Photonics*, 2nd ed. Hoboken, NJ, USA: Wiley, 2007, ch. 10, pp. 365–400.
[29] G. M. Hale and M. R. Querry, "Optical constants of water in the 200-nm to 200-μm wavelength region," *Appl. Opt.*, vol. 12, no. 3, pp. 555–563, 1973.
[30] M. Aas *et al.*, "FRET lasing from self-assembled DNA tetrahedral nanostructures suspended in optofluidic droplet resonators," *Eur. Phys. J., Spec. Topics*., vol. 223, no. 10, pp. 2057–2062, Sep. 2014.
[31] E. Özelci, M. Aas, A. Jonáš, and A. Kiraz, "Optofluidic FRET microlasers based on surface-supported liquid microdroplets," *Laser Phys. Lett.*, vol. 11, no. 4, p. 045802, Apr. 2014.

Mehdi Aas received the B.S. and M.S. degrees in physics from the University of Tabriz, Tabriz, Iran, and Shahid Beheshti University, Tehran, Iran, in 2002 and 2005, respectively. Since 2011, he has been working toward the Ph.D. degree at Koç University, Istanbul, Turkey. From 2006 to 2011, he was an Instructor with the University of Bonab.

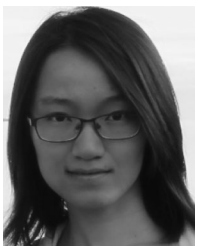

Qiushu Chen received the B.S. degree in physics from Peking University, Beijing, China, in 2012. She is currently working toward the Ph.D. degree in biomedical engineering at the University of Michigan, Ann Arbor, MI, USA. Her research interests include optofluidic lasers and its biomedical applications.

Alexandr Jonáš received the M.S. degree in biophysics from Masaryk University, Brno, Czech, in 1996, and the Ph.D. degree in physical and material engineering from the Brno University of Technology, Brno, in 2001. From 2002 to 2003, he was a Postdoctoral Researcher with the European Molecular Biology Laboratory, Heidelberg, Germany, and from 2004 to 2006 with the University of Texas, Austin, TX, USA. In 2007, he joined the Institute of Scientific Instruments, Brno, and worked on combining optical micromanipulation techniques with Raman spectroscopy. Between 2010 and 2013, he was a Marie Curie/TUBITAK Research Fellow with Koç University, Istanbul, Turkey, studying optical properties of microdroplet-based resonators. He is currently an Assistant Professor at the Department of Physics, Istanbul Technical University, Istanbul. His research interests include the development and applications of optical micromanipulation, microscopy, and spectroscopy techniques for characterization of complex environments.

Alper Kiraz received the B.S. degree in electrical-electronics engineering from Bilkent University, Ankara, Turkey, in 1998, and the M.S. and Ph.D. degrees in electrical and computer engineering from the University of California, Santa Barbara, CA, USA, in 2000 and 2002, respectively. Between 2002 and 2004, he was a Postdoctoral Associate with the Institute for Physical Chemistry, Ludwig-Maximilians University, Munich, Germany, and received the Alexander von Humboldt Fellowship. He joined Koç University and became a Full Professor in 2014. Between 2014 and 2015, he was a Visiting Professor of biomedical engineering at the University of Michigan, Ann Arbor, MI, USA, as a Fulbright Fellow. His current research interests include optofluidics, single-molecule spectroscopy/microscopy, optical manipulation, and biomedical instrumentation. His research team worked with various research projects targeting the development of novel microoptical devices, optofluidic lab-on-a-chip devices, molecular and gas sensors, optofluidic-based renewable energy solutions, and confocal microscope device concepts.

Xudong Fan received the B.S. and M.S. degrees from Peking University, Beijing, China, in 1991 and 1994, respectively, and the Ph.D. degree in physics and optics from the Oregon Center for Optics, University of Oregon, Eugene, OR, USA, in 2000. Between 2000 and 2004, he was a Project Leader with 3M Company on fiber optics and photonic sensing devices for biomedical applications. In 2004, he joined the Department of Biological Engineering, University of Missouri as an Assistant Professor and was promoted to Associate Professor in 2009. In January 2010, he joined the Biomedical Engineering Department, University of Michigan, Ann Arbor, MI, USA, where in 2014, he was promoted to a Full Professor. His research interests include the interface of photonics, micro/nanofluidics, nano-/biotechnologies, and biomedicine. He was an Associate Editor of the *Optics Express* between 2008 and 2014. He is currently with the Editorial Board of Lab on a Chip for the Royal Society of Chemistry.